Anomalous Diffusion Probes Microstructure Dynamics of Entangled F-Actin Networks

I. Y. Wong,[1] M. L. Gardel,[1] D. R. Reichman,[2] Eric R. Weeks,[3] M. T. Valentine,[1] A. R. Bausch,[4] and D. A. Weitz[1]

[1]*Department of Physics & DEAS, Harvard University, Cambridge, Massachusetts 02138, USA*
[2]*Department of Chemistry and Chemical Biology, Harvard University, Cambridge, Massachusetts 02138, USA*
[3]*Department of Physics, Emory University, Atlanta, Georgia 30322, USA*
[4]*Lehrstuhl für Biophysik - E22, Technische Universität München, Garching, Germany*

We study the thermal motion of colloidal tracer particles in entangled actin filament (F-actin) networks, where the particle radius is comparable to the mesh size of the F-actin network. In this regime, the ensemble-averaged mean-squared displacement of the particles is proportional to τ^γ, where $0 < \gamma < 1$ from $0.1 < \tau < 100$ s and depends only on the ratio of the probe radius to mesh size. By directly imaging hundreds of particles over 20 min, we determine this anomalous subdiffusion is due to the dynamics of infrequent and large jumps particles make between distinct pores in the network.

The cytoskeleton is composed of dense actin filament (F-actin) networks that regulate many important cellular processes such as cell shape, motility, and division [1]. The mechanical properties of these networks control proper biological function, but these mechanical properties are challenging to measure *in vivo* and are difficult to model theoretically as the details of cytoskeletal microstructure are not well understood [2,3]. This has motivated an extensive effort to measure the mechanical properties and microstructure of reconstituted F-actin networks *in vitro* [4–9]. F-actin is a semiflexible polymer, which is characterized by a persistence length of 10–20 μm, roughly 3 orders of magnitude larger than the filament diameter of 7 nm [10,11]. *In vitro*, the contour length of F-actin filaments is typically greater than 20 μm, and semidilute solutions of actin form entangled networks of semiflexible polymers with an average mesh size, ξ, of order 100 nm to 1 μm. Thus, solutions of entangled F-actin are an ideal model system with which to study the unique dynamics and mechanical properties of semiflexible polymer networks and to investigate the implications of the underlying mechanisms of these properties for the behavior of the cytoskeleton.

The unique mechanical properties of F-actin networks are determined by structures and dynamics on the scale of microns. Thus, full elucidation of these properties demands techniques that probe the behavior at these length scales; this has inspired the development of microrheological methods, where the motion of micron-sized tracer particles, driven by thermal, magnetic, or optical forces, is used to make precise local measurements of viscosity and mechanical properties at the length scale of the tracer particle [4–9,12–14]. When the particle radius, a, is much smaller than ξ, the one-dimensional mean-squared displacement (MSD), $\langle \Delta x^2(\tau) \rangle$, of the tracer, particles evolves linearly in time, $\langle \Delta x^2(\tau) \rangle = 2D\tau$. In this case, the particle motion is sensitive to the local viscosity of the solvent and reflects the effect of macromolecular crowding [15,16] as well as hydrodynamic

interactions with the network [5,17], both of which decrease the measured diffusion constant, D. By contrast, when a is larger than ξ, the particles are constrained by the surrounding polymer network, and the bead motions directly reflect the local elasticity of the network [6,8,14]. In the intermediate case, when $a \approx \xi$, the particle motion should directly probe the network dynamics and mechanics at the scale of a, the critical length scale for important network properties; unfortunately, very little is known about particle motion when $a \approx \xi$.

In this Letter, we show that particle motion in F-actin networks with $a \approx \xi$ does indeed directly reflect the dynamics of the local microstructure of the network. The ensemble-averaged MSD of particles exhibits anomalous subdiffusive behavior, $\langle \Delta x^2(\tau) \rangle \sim \tau^\gamma$, where $0 < \gamma < 1$, over a wide range of lag times, τ. Remarkably, the diffusive exponent, γ, is a function only of the ratio of the particle radius to the mesh size and can be tuned from one to zero over a narrow range $0.42 < a/\xi < 1.25$. This subdiffusive behavior is due to the surprising dynamics of individual particles; they remain trapped within a localized "cage" of actin filaments, but can infrequently "jump" between different cages. The temporal distribution of these jumps results in the anomalous subdiffusion and reveals new insights into the length scale dependent dynamics of the entangled F-actin microstructure.

Lyophilized G-actin is dissolved in deionized water, dialyzed against fresh G-buffer (2 mM Tris-HCl, 0.2 mM ATP, 0.2 mM CaCl$_2$, 0.2 mM DTT, 0.005% NaN$_3$, pH 8.0) at 4 °C for 24 h and used within 7 days of preparation. G-actin is mixed with carboxylate modified colloidal spheres with radius $a = 0.25$ μm and polymerized by gently mixing with 1/10 of the final sample volume of 10x F-buffer (20 mM Tris-HCl, 20 mM MgCl$_2$, 1 M KCl, 2 mM DTT, 2 mM CaCl$_2$, 5 mM ATP, pH 7.5). The mesh size in microns is $\xi = 0.3/\sqrt{c_A}$ [4], where the actin concentration c_A is measured in mg/mL. Modifying the bead surface chemistry to prevent total protein adsorption has small effects on the overall particle mobility [8], but

does not qualitatively affect our results. The sample is loaded into a glass sample chamber, sealed with vacuum grease, and equilibrated under constant rotation for 1 h at $\sim 25\,^\circ\mathrm{C}$. We image approximately 100 particles using bright field microscopy and follow their dynamics with a charge-coupled device camera (30 images/s, 1/2000 s shutter) for 4–30 min [18]. We focus 100 μm into the sample to avoid wall effects. Particle centers are found in each image to an accuracy of 20 nm, and particle trajectories are determined [19] to calculate the ensemble-averaged MSD $\langle \Delta x^2(\tau) \rangle$.

We observe dramatically different temporal dependence of the MSD as a/ξ is varied. When $a > \xi$, the particle is tightly confined by the local elasticity of the network, and its thermal motion can then be interpreted using the framework of microrheology [6,12] to provide a direct measure of the plateau shear modulus, although the full frequency dependence of the modulus is not captured by the thermal motion of a single particle [14]. For example, in an F-actin network with $\xi = 0.17$, the MSD of 0.25 μm particles is approximately constant between 0.01 and 10 s, as shown by the open squares in Fig. 1; this corresponds to an elastic modulus of 2 Pa, which is consistent with the elastic plateau modulus measured with bulk rheology [20]. By contrast, if $a \ll \xi$, the particle can diffuse freely, and the diffusion coefficient D can be used to probe the viscosity of the background fluid of the network. For F-actin with $\xi = 0.75$, the MSD of 0.25 μm spheres evolves nearly linearly in time between 0.01 and 10 s, as shown by the open triangles in Fig. 1. This corresponds to a solvent viscosity of 1.5 cP, slightly larger than the viscosity of pure water, presumably reflecting the effects of hydrodynamic interactions with the actin network [5]. However, when a is comparable to ξ, dramatically different behavior is observed. The MSD exhibits anomalous subdiffusion, increasing as a power law for large times, $\langle \Delta x^2(\tau) \rangle \sim \tau^\gamma$, where the exponent γ depends on the ratio of the particle radius a to the mesh size ξ, as shown by the solid symbols in Fig. 1. The
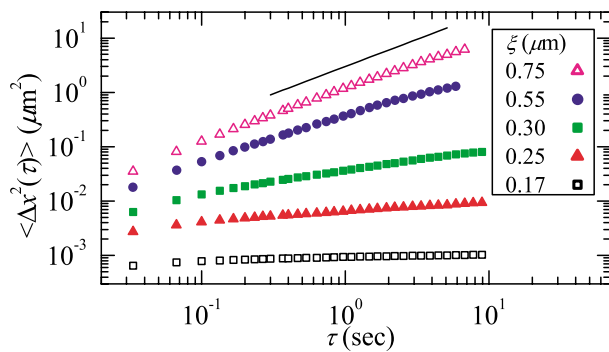
motion of earlier lag times is also subdiffusive, albeit with a slightly larger exponent. Interpreting this anomalous diffusion using microrheological analysis yields a viscoelastic response, whose magnitude and frequency dependence are in sharp disagreement with bulk measurements. Thus, the MSD does not provide an accurate or robust measure of the viscoelasticity and must reflect alternate microscopic particle dynamics.

To elucidate the origin of these subdiffusive MSDs, we exploit the advantages of multiple particle tracking [18] and examine the spatial trajectories of individual tracers in 0.9 mg/mL F-actin, where $a/\xi = 0.83$ for times up to 30 min. The majority of the particles are highly constrained by the network, and their trajectories exhibit fluctuations with nearly Gaussian statistics, as illustrated by the spatial and temporal trajectories shown in Figs. 2(a) and 2(b), respectively. If the ensemble average is restricted to these constrained particles, the MSD approaches a plateau at times longer than 0.4 s, as shown by the solid curve in Fig. 3(a); using the microrheology formalism yields an elastic plateau modulus of 0.15 Pa, consistent with bulk measurements [20]. However, roughly 20% of the particles exhibit remarkably different dynamics. These particles undergo constrained motion punctuated by large scale jumps, as illustrated by the spatial and temporal trajectories in Figs. 2(c) and 2(d). The time scale of these jumps is very short compared to the residence time within the cages. This suggests that the particles randomly and rapidly jump between different microenvironments wherein they are constrained. Within these local environments, the MSD exhibits the same time dependence as that of the majority of the particles which do not display these jumps, as shown by the open circles in Fig. 3(a), which is the MSD calculated exclusively from the constrained motion, ignoring the jumps. Thus, the viscoelastic properties of these constraining microenvironments are the same as those of the rest of the network. However, when the MSD is ensemble averaged over all particles, including the jumps, the power-law dependence is recovered, as shown by the solid
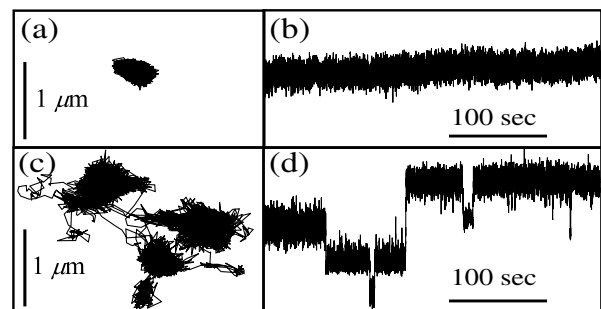

FIG. 1 (color online). MSD of 0.25 μm spheres in F-actin with $\xi = 0.79$ μm (open triangles), 0.55 μm (solid circles), 0.30 μm (solid squares), 0.25 μm (solid triangles), and 0.17 μm (open squares). The solid line indicates a linear fit, $\langle \Delta x^2(\tau) \rangle \sim \tau$.

FIG. 2. (a) Representative constrained x-y trajectory of a 0.25 μm particle in 0.9 mg/mL ($\xi = 0.31$ μm) F-actin over 600 s. (b) The y coordinate of (a) as a function of time. (c) Representative jumping x-y trajectory from same sample. (d) The y coordinate in (c) as a function of time.
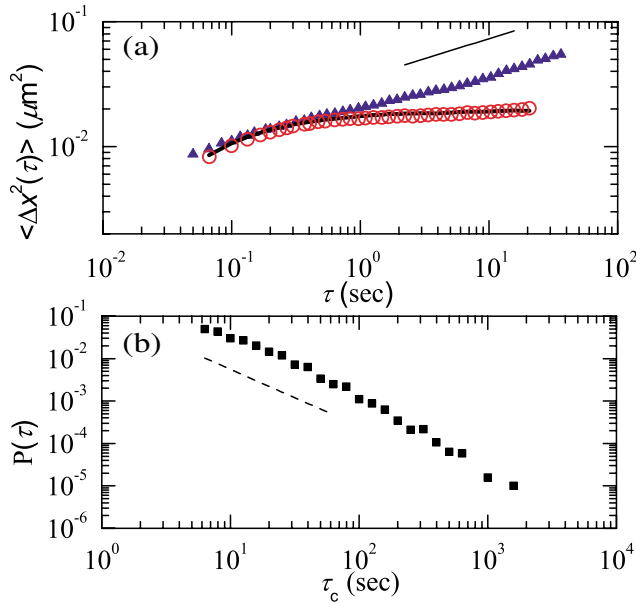
FIG. 3 (color online). (a) MSD of 0.25 μm particles in
0.9 mg/mL F-actin (triangles). The solid line indicates a
power-law fit τ^{γ}, where $\gamma = 0.32$. The MSD of constrained
particles (line) and caged portions of jumping particles (open
circles) agree well. (b) Histogram of cage times for jump-
ing 0.25 μm particles in 0.9 mg/mL F-actin (squares). The
dashed line indicates a power-law fit, $P(\tau_c) \sim \tau_c^{-\nu}$, with
$\nu = 1.33 \pm 0.04$.

triangles in Fig. 3(a). Thus, the anomalous diffusion re-
sults from the dynamics of the jumps between local
microenvironments.

In order to quantify these dynamics, we determine
the probability distribution of cage times τ_c within the
local microenvironments. For large cage times, this
probability distribution function scales as a power law
$P(\tau_c) = A\tau_c^{-\nu}$, as shown in Fig. 3(b). The normalization
constant, A, is determined using the minimum cutoff
time necessary for sufficient statistics. To model this
motion, we assume that the particle undergoes a random
walk, but, unlike normal diffusive motion, the time scale
of each step is chosen from a power-law distribution
$P(\tau_c) \sim \tau_c^{-\nu}$. When the steps are chosen symmetrically
and $1 < \nu < 2$, this model predicts that the MSD should
be subdiffusive, scaling asymptotically as $\gamma = \nu - 1$ for
uncorrelated jumps [21]. This relationship is in good
agreement with our data for 0.25 μm spheres in
0.9 mg/mL F-actin, as shown by the power-law fit of $\gamma =
0.32$ to the MSD in Fig. 3(a) and the power-law fit of $\nu =
1.33$ to the probability distribution function of waiting
times in Fig. 3(b). Similar good agreement is obtained for
other actin concentrations. A consequence of such a
power-law distribution is that the mean cage time is not
well defined, consistent with our observation that a ma-
jority of the particles remain constrained over the obser-
vation time.

The ensemble-averaged MSD of the tracers can di-
rectly reveal the dynamical microstructure of the en-

tangled actin network. To illustrate this, we determine
the MSD of 0.25 μm particles over a large range of actin
concentrations. The exponent characterizing the subdif-
fusive motion γ changed smoothly with the ratio of the
particle radius a to the mesh size ξ, as shown by the open
squares in Fig. 4. By using several different sized tracer
particles varying from 0.25–0.5 μm, we find that γ de-
pends only on the ratio of the bead size to the mesh size,
rather than the actual bead radius or actin concentration
as shown in Fig. 4. Over a very narrow range, $0.42 <
a/\xi < 1.25$, we observe anomalous subdiffusion with γ
decreasing rapidly as a function of a/ξ. The steep de-
crease of γ in this range shows that even small variations
in a or in ξ can have large effects on the bead mobility in
a network. These results strikingly demonstrate that the
actin network is inhomogeneous and that the subdiffusive
motion is traplike; thus, interpreting the MSD within the
framework of microrheology must be done with extreme
care for these particles. Instead, the particle motion re-
flects the dynamics of the network on length scales
comparable to the particle size.

While the residence time in the traps or pores is very
long, jumps between pores are rapid; their time scale is
~0.5 s, while the distance between pores is ~1 μm. If the
transport between pores were diffusive, the jump time
would be ~$(1\ \mu m)^2/D \approx 2$ s. Thus, the motion between
pores may be diffusive in nature or, alternatively, the
particle may be actively pushed into the new pore by a
release of elastic energy of filaments in the network.

The anomalous subdiffusion of the MSD is reminiscent
of the power-law fluctuations of individual actin filaments
[7]; however, any model for the particle motion that is
restricted to such fluctuations cannot account for the
dependence of the exponent on a/ξ. To describe this
intermittent motion within a general framework, we for-
mulate a model similar to that used to describe activation
over a free energy barrier. We assume that the jumps
between microenvironments are driven by elastic forces
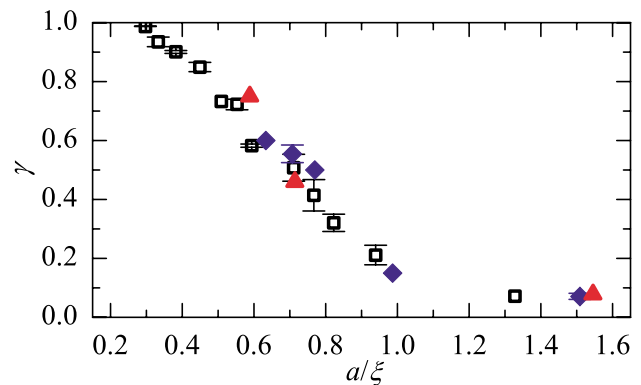and are uncorrelated. Then, the waiting time distribution

FIG. 4 (color online). The scaling of the diffusive exponent,
γ, as a function of a/ξ for several particle radii, a: 0.25 μm
(open squares), 0.32 μm (diamonds), and 0.5 μm (triangles).
Error bars indicate measured sample-to-sample variation.

can be calculated as [22]

$$P(\tau) \propto -\frac{d}{d\tau}\langle\theta(\mathcal{F}(\tau) - \mathcal{F}_0)\theta(\mathcal{F}(0) - \mathcal{F}_0)\rangle, \quad (1)$$

where $\mathcal{F}$ reflects the net magnitude of the force acting to push the tracer particle out of the local microenvironment, and $\theta(\mathcal{F}(\tau) - \mathcal{F}_0)$ is a step function that counts only jumping events if the parameter $\mathcal{F}$ has exceeded a threshold value $\mathcal{F}_0$. Using the spectral representation of $\theta(x)$ [23], an analytical expression for $P(\tau)$ can be obtained within the second cumulant approximation for the correlations of $\mathcal{F}(\tau)$; this behaves asymptotically as $P(\tau) \propto -\frac{d}{d\tau}\langle\mathcal{F}(\tau)\mathcal{F}(0)\rangle$. We assume the elastic forces arise from coupling between the particle and the transverse fluctuations of the actin filaments in the network; since these have power-law correlations over time scales below ~ 1 s [6,7], we assume that $\mathcal{F}(\tau)$ also has power-law correlations, $\langle\mathcal{F}(\tau)\mathcal{F}(0)\rangle \sim \tau^{-\alpha}$, and thus $\nu = \alpha + 1$.

Despite the absence of precise information about the correlations of $\mathcal{F}$, several qualitative conclusions can nevertheless be made. The exponent α will decrease as the ratio of bead diameter to mesh size increases, since the larger size of the probe locally cuts off small length scales and rapid fluctuations; thus, α will vary continuously. By contrast, microrheological models that relate subdiffusion to the elastic properties of the underlying network would not display this behavior [12]. In addition, we would expect the exponent α to be relatively temperature insensitive, so the temperature dependence of the subdiffusive exponent should be weaker than that predicted by trap models based on activation over a broad distribution of energy barriers [24]. The transport behavior we observe may help account for rheological measurements of cells [25] which have been interpreted in terms of the "soft glassy rheology" model [26]. In this model, the standard temperature is replaced with an effective noise temperature, χ. Our experiments suggest that χ may be connected to the elastic energy stored locally in the actin network and thus related to the decay of the correlations of $\mathcal{F}(\tau)$.

These results suggest that particle motions must be interpreted carefully, especially in materials where the structural length scale or dynamics are not well known. A judicious choice of particle sizes and concentrations can probe the dynamics of the surrounding entangled actin network on varying length scales, yielding information about the network elasticity, solvent viscosity, and microstructure dynamics. Moreover, such cage-jumping behavior may also have implications for understanding the transport of proteins and macromolecular solutes through "crowded" cytoskeletal environments.

---

[1] B. Alberts, D. Bray, A. Johnson, J. Lewis, M. Raff, K. Roberts, and P. Walter, *Essential Cell Biology* (Garland, New York, 2002).

[2] J. Howard, *Mechanics of Motor Proteins and the Cytoskeleton* (Sinauer, Sunderland, 2001).

[3] D. Boal, *Mechanics of the Cell* (Cambridge University Press, New York, 2002).

[4] C. F. Schmidt, M. Barmann, G. Isenberg, and E. Sackmann, Macromolecules **22**, 3638 (1989).

[5] J. D. Jones and K. LubyPhelps, Biophys. J. **71**, 2742 (1996).

[6] B. Schnurr, F. Gittes, F. C. MacKintosh, and C. F. Schmidt, Macromolecules **30**, 7781 (1997).

[7] F. Amblard, A. C. Maggs, B. Yurke, A. N. Pargellis, and S. Leibler, Phys. Rev. Lett. **77**, 4470 (1996).

[8] J. McGrath, J. Hartwig, and S. Kuo, Biophys. J. **79**, 3258 (2000).

[9] T. Gisler and D. A. Weitz, Phys. Rev. Lett. **82**, 1606 (1999).

[10] A. Ott, M. Magnasco, A. Simon, and A. Libchaber, Phys. Rev. E **48**, R1642 (1993).

[11] F. Gittes, B. Mickey, J. Nettleton, and J. Howard, J. Cell Biol. **120**, 923 (1993).

[12] T. G. Mason and D. A. Weitz, Phys. Rev. Lett. **74**, 1250 (1995).

[13] T. G. Mason, K. Ganesan, J. H. van Zanten, D. Wirtz, and S. C. Kuo, Phys. Rev. Lett. **79**, 3282 (1997).

[14] F. G. Schmidt, B. Hinner, and E. Sackmann, Phys. Rev. E **61**, 5646 (2000).

[15] A. S. Verkman, Trends Biochem. Sci. **27**, 27 (2002).

[16] A. P. Minton, J. Bio. Chem. **276**, 10 577 (2001).

[17] D. S. Clague and R. J. Phillips, Phys. Fluids **8**, 1720 (1996).

[18] M. T. Valentine, P. D. Kaplan, D. Thota, J. C. Crocker, T. Gisler, R. K. Prud'homme, M. Beck, and D. A. Weitz, Phys. Rev. E **64**, 061506 (2001).

[19] J. C. Crocker and D. G. Grier, J. Colloid Interface Sci. **179**, 298 (1996).

[20] B. Hinner, M. Tempel, E. Sackmann, K. Kroy, and E. Frey, Phys. Rev. Lett. **81**, 2614 (1998).

[21] E. R. Weeks, J. S. Urbach, and H. L. Swinney, Physica (Amsterdam) **97D**, 291 (1996).

[22] P. Bolhuis, D. Chandler, C. Dellago, and P. Geissler, Annu. Rev. Phys. Chem. **53**, 291 (2002).

[23] A. Stuchebrukhov, J. Chem. Phys. **95**, 4258 (1991).

[24] C. Monthus and J.-P. Bouchaud, J. Phys. A **29**, 3847 (1996).

[25] B. Fabry, G. Maksym, J. Butler, M. Glogauer, D. Navjas, and J. Fredberg, Phys. Rev. Lett. **87**, 148102 (2001).

[26] P. Sollich, F. Lequeux, P. Hebraud, and M. Cates, Phys. Rev. Lett. **78**, 2020 (1997).